Brain Advance Access published March 14, 2012
doi:10.1093/brain/aws059 Brain 2012: Page 1 of 10 | 1
BRAIN
A JOURNAL OF NEUROLOGY

Identifying major depression using whole-brain functional connectivity: a multivariate pattern analysis

Ling-Li Zeng,[1,*] Hui Shen,[1,*] Li Liu,[2,*] Lubin Wang,[1] Baojuan Li,[1] Peng Fang,[1] Zongtan Zhou,[1] Yaming Li[3] and Dewen Hu[1]

1 College of Mechatronics and Automation, National University of Defense Technology, Changsha, Hunan 410073, People's Republic of China
2 Department of Psychiatry, First Affiliated Hospital, China Medical University, Shenyang, Liaoning, 110001, People's Republic of China
3 Department of Nuclear Medicine, First Affiliated Hospital, China Medical University, Shenyang, Liaoning, 110001, People's Republic of China

*These authors contributed equally to this work.

Correspondence to: Professor Dewen Hu,
College of Mechatronics and Automation,
National University of Defense Technology,
Changsha, Hunan 410073,
People's Republic of China
E-mail: dwhu@nudt.edu.cn

Recent resting-state functional connectivity magnetic resonance imaging studies have shown significant group differences in several regions and networks between patients with major depressive disorder and healthy controls. The objective of the present study was to investigate the whole-brain resting-state functional connectivity patterns of depressed patients, which can be used to test the feasibility of identifying major depressive individuals from healthy controls. Multivariate pattern analysis was employed to classify 24 depressed patients from 29 demographically matched healthy volunteers. Permutation tests were used to assess classifier performance. The experimental results demonstrate that 94.3% ($P < 0.0001$) of subjects were correctly classified by leave-one-out cross-validation, including 100% identification of all patients. The majority of the most discriminating functional connections were located within or across the default mode network, affective network, visual cortical areas and cerebellum, thereby indicating that the disease-related resting-state network alterations may give rise to a portion of the complex of emotional and cognitive disturbances in major depression. Moreover, the amygdala, anterior cingulate cortex, parahippocampal gyrus and hippocampus, which exhibit high discriminative power in classification, may play important roles in the pathophysiology of this disorder. The current study may shed new light on the pathological mechanism of major depression and suggests that whole-brain resting-state functional connectivity magnetic resonance imaging may provide potential effective biomarkers for its clinical diagnosis.

Keywords: major depression; multivariate pattern analysis; functional MRI; functional connectivity; resting state

Received May 13, 2011. Revised December 31, 2011. Accepted January 3, 2012.

Introduction

Major depressive disorder is a common mental illness characterized by a persistent, pervasive depressed mood or anhedonia, a sense of worthlessness and cognitive impairments. Up to 10% of people with depressive episodes will become suicidal if untreated (APA, 2000). To date, the diagnosis of major depression has largely been based on self-reported symptoms and clinical signs. Understanding the pathophysiology of major depression is clearly an international imperative.

It has been proposed that major depressive symptoms are associated with the dysregulation of a distributed neuronal network encompassing cortical and limbic regions rather than with the (functional) breakdown of a single discrete brain region (Mayberg, 1997, 2003; Davidson *et al*., 2002; Drevets, 2003; Phillips *et al*., 2003; Seminowicz *et al*., 2004; Drevets *et al*., 2008; Price and Drevets, 2010). Recently, resting-state functional MRI has attracted increasing attention for mapping large-scale neural network function and dysfunction. During rest, low-frequency (0.01–0.08 Hz) blood oxygen level-dependent fluctuations of functional MRI signals are thought to be related to spontaneous neuronal activity, and the correlation analysis method has proven effective for measuring functional connectivity network alterations in neuropsychiatric conditions, including depression (Greicius *et al*., 2007; Greicius, 2008; Buckner, 2010). The tonic nature of major depressive core symptoms indicates that resting-state functional MRI may be helpful for improving our understanding of the pathophysiological mechanisms underlying affective and cognitive dysfunctions in major depression (Mesulam, 1998; Van den Heuvel and Hulshoff Pol, 2010). Based on resting-state functional MRI, a growing body of studies has focused on the quantitative analysis of the brains of patients with neurological and psychiatric disorders, including Alzheimer's disease and dementia (Greicius *et al*., 2004; Zhou *et al*., 2010*a*), and schizophrenia (Liu *et al*., 2008*b*; Whitfield-Gabrieli *et al*., 2009). Using seed-based methods, resting-state functional MRI studies have detected network alterations in depressed patients, especially abnormalities in the default mode network and the affective network (Anand *et al*., 2005, 2009; Greicius *et al*., 2007; Bluhm *et al*., 2009; Sheline *et al*., 2010; Zhou *et al*., 2010*b*). Similarly, Craddock *et al*. (2009) employed multivoxel pattern analysis to predict major depressive state using resting-state functional connectivity limited to 15 predefined regions of interest. Veer *et al*. (2010) extracted resting-state networks of depressed patients using independent component analysis, and then used univariate statistical methods to investigate the identified components. These studies provide valuable insight into the pathological mechanism of major depression, but they also have some significant limitations. First, seed-based methods limit the obtained information to the selected regions of interest and make it difficult to examine functional connectivity patterns on a whole-brain scale (Van den Heuvel and Hulshoff Pol, 2010). Secondly, traditional group-level statistical methods do not provide a mechanism for evaluating the discriminative power of the identified connections at the individual level (Seidman *et al*., 2004; Craddock *et al*., 2009).

As a data-driven technique, multivariate pattern analysis based on whole-brain resting-state functional MRI data can complement both seed-based and univariate statistical analyses. Whole-brain functional connectivity analysis, unlike those analysing several predefined regions or networks of interest, can ensure the optimal use of the wealth of information present in the brain imaging data. In particular, multivariate pattern analysis methods can both find potential neuroimaging-based biomarkers to differentiate patients from healthy controls at the individual subject level and potentially detect exciting spatially distributed information to further highlight the neural mechanisms underlying the behavioural symptoms of major depression (Pereira *et al*., 2009). In recent years, there has been increasing interest in multivariate pattern analysis methods to categorize psychiatric patients from healthy controls using structural or functional brain images (Klöppel *et al*., 2008; Craddock *et al*., 2009; Desikan *et al*., 2009; Shen *et al*., 2010; Zhou *et al*., 2010*a*; Ardekani *et al*., 2011). If a multivariate pattern analysis-based classifier can label new samples with better-than-random accuracy, then the two populations are indeed likely to be different, and the classifier can capture the population differences (Golland and Fischl, 2003). In multivariate pattern analysis-based brain imaging analysis, the features for classification can be various structural characteristics or functional properties extracted from neuroimaging data. For resting-state functional MRI, resting-state functional connectivity measured by the correlation of two functional MRI time series has been used for the discrimination of psychiatric disorders (Craddock *et al*., 2009; Shen *et al*., 2010).

To date, it is unknown whether multivariate pattern analysis can capture whole-brain resting-state functional connectivity patterns to discriminate or identify depressed patients from healthy controls at the individual subject level with a high degree of accuracy. The purpose of this study was to explore significant disorder-related patterns using whole-brain resting-state functional MRI in medication-free depressed patients without co-morbidity and in carefully matched healthy controls and to discriminate patients from healthy subjects. The altered functional connections were expected to be observed in the resting-state networks that include areas known to be associated with affective and cognitive processing. Functional connectivity, measured by the correlation of two activity time series of anatomically separated brain regions, was used as a classification feature. This exploration will be helpful in further discovering the neural mechanisms underlying the behavioural symptoms of depression, which may offer additional information for advancing our understanding of the pathophysiology of this disorder.

Materials and methods

Subjects

The study's participants included 32 patients diagnosed with major depressive disorder from the outpatient clinic at the First Affiliated Hospital of China Medical University and 33 demographically similar healthy volunteers recruited through advertisements. All of the subjects were right-handed native Chinese speakers. Three patients and two controls were removed from the sample due to excessive head

Table 1 Characteristics of the participants in this study

Variable	Mean ± SD (range)		*P*-value
	Patient	Control	
Sample size	24	29	
Gender (male/female)	8/16	9/20	0.86[a]
Age (years)	31.83 ± 10.99 (18–52)	33.62 ± 10.29 (19–53)	0.54[b]
Education (years)	11.71 ± 3.13	11.00 ± 3.12	0.66[b]
Weight (kg)	60.5 ± 10.93	62.55 ± 8.59	0.45[b]
Age of illness onset (years)	28.71 ± 10.90		
Number of previous episodes	1.63 ± 0.77		
Duration of current episode (months)	5.33 ± 6.29 (1–24)		
Hamilton Depression Rating Scale	26.42 ± 5.22 (18–38)	4.25 ± 1.02 (3–6)	
Hamilton Anxiety Rating Scale	20.29 ± 5.25 (8–30)	3.55 ± 0.91 (2–5)	
Clinical Global Impression Scale-Severity	5.92 ± 0.65 (5–7)		

[a]Pearson Chi-square test.
[b]Two-sample *t*-test.

motion during scan acquisition (>2.5 mm translation and/or >2° rotation). Five additional patients and two additional control subjects were removed due to head motions with acute fluctuations that caused strong spurious correlation. The remaining 24 depressed patients and 29 healthy controls remained gender-, age-, education- and weight-matched (see Table 1).

Depressed patients met the criteria for a current episode of unipolar recurrent major depression based on the DSM (Diagnostic and Statistical Manual of Mental Disorders)-IV criteria (APA, 2000). Using the Structured Clinical Interview for DSM-IV (First *et al.*, 1995), confirmation of the diagnosis was made by clinical psychiatrists. All patients were medication-naive at the time of the scan. Exclusion criteria included acute physical illness, substance abuse or dependence, a history of head injury resulting in loss of consciousness and major psychiatric or neurological illness other than depression. Similar exclusion criteria were adopted for healthy control subjects. On the days of the scans, the depressive symptoms of patients were assessed with the 17-item Hamilton Depression Rating Scale (Hamilton, 1960), Hamilton Anxiety Rating Scale (Hamilton, 1959) and Clinical Global Impression Scale-Severity (Guy, 1976) (see Table 1). Healthy volunteer subjects were studied under identical conditions. This study was approved by the Ethics Committee of the First Affiliated Hospital of China Medical University, and all participants gave written informed consent.

Resting experiment and image acquisition

In the experiments, subjects were simply instructed to keep their eyes closed, relax, remain awake and perform no specific cognitive exercise. After each session, subjects were asked whether they were awake and relaxed in the previous session, and all of the subjects confirmed that they were. Magnetic resonance images were acquired using a 1.5-T GE SIGNA scanner (GE Medical Systems). To reduce head movement, the subjects' heads were fixed using foam pads with a standard birdcage head coil. All functional MRI images were collected using a gradient-echo echo planar imaging sequence. The imaging parameters were as follows: repetition time/echo time = 2000/50 ms, thickness/gap = 5/1.5 mm, field of view = 240 mm × 240 mm, flip angle = 90°, matrix = 64 × 64 and slices = 20. Each functional resting-state session lasted ~8 min, and 245 volumes were obtained.

Data preprocessing

Resting-state functional MRI images were preprocessed using a statistical parametric mapping software package (SPM5®, http://www.fil.ion.ucl.ac.uk/spm). For each subject, the first five volumes of the scanned data were discarded for magnetic saturation. The remaining 240 volumes were corrected by registering and re-slicing for head motion. Next, the volumes were normalized to the standard echo planar imaging template in the Montreal Neurological Institute space. The resulting images were spatially smoothed with a Gaussian filter of 8 mm full-width half-maximum kernel, detrended to abandon linear trend and then temporally filtered with a Chebyshev band-pass filter (0.01–0.08 Hz). The registered functional MRI volumes with the Montreal Neurological Institute template were divided into 116 regions according to the automated anatomical labelling atlas (Schmahmann *et al.*, 1999; Tzourio-Mazoyer *et al.*, 2002). The atlas divides the cerebrum into 90 regions (45 in each hemisphere) and divides the cerebellum into 26 regions (nine in each cerebellar hemisphere and eight in the vermis). All region of interest masks were generated using the free software WFU_PickAtlas® (version 2.0, http://www.ansir.wfubmc.edu) (Maldjian *et al.*, 2003).

Regional mean time series were obtained for each individual by averaging the functional MRI time series over all voxels in each of the 116 regions. Note that aside from the band-pass filtering and correcting for movement, additional preprocessing steps, such as global signal regression, have recently been performed in functional connectivity analysis (Fox *et al.*, 2009). Global signal regression creates artefactual negative correlations, but this technique is suggested to improve the specificity of positive correlations and can remove specific confounds from the data to facilitate the evaluation of neurophysiological relationships (Fox *et al.*, 2009), so the results with global signal regression are more readily or reliably interpreted. Therefore, each regional mean time series was further corrected by regressing out head motion and the global signals. To further reduce spurious variance unlikely to reflect neuronal activity, we have included in the regression the white matter and cerebrospinal fluid (CSF) average signals, as well as the first order derivative terms for the global, white matter and CSF average signals (Fox *et al.*, 2006; Fair *et al.*, 2008; Biswal *et al.*, 2010; Dosenbach *et al.*, 2010). The time courses of noise components extracted by using group independent component analysis were also utilized for artefact removal for each subject (Liu *et al.*, 2008a; Kelly *et al.*, 2010). The residuals of these regressions

constituted the set of regional mean time series used for functional connectivity analyses. We evaluated functional connectivity between each pair of regions using Pearson correlation coefficient. Thus, for each subject, we obtained a resting-state functional network captured by a 116×116 symmetric matrix. Removing 116 diagonal elements, we extracted the upper triangle elements of the functional connectivity matrix as classification features, i.e. the feature space for classification was spanned by the $(116 \times 115)/2 = 6670$ dimensional feature vectors.

Identification of features with high discriminative power

The abnormal resting-state functional connectivity patterns in depression are principally represented by the highly discriminating functional connections, and initially reducing the number of features accelerates computation and diminishes noise (Pereira *et al.*, 2009; Dosenbach *et al.*, 2010; Shen *et al.*, 2010). Therefore, feature selection was used to construct the feature space for classification by retaining the most discriminating functional connections and eliminating the rest. The discriminative power of a feature can be quantitatively measured by its relevance to classification (Guyon and Elisseeff, 2003). In this study, we used the Kendall tau rank correlation coefficient (Kendall and Jean, 1990), which provides a distribution-free test of independence between two variables to measure the relevance of each feature to classification.

Suppose that there are m samples in the patient group and n samples in the control group. Let x_{ij} denote the functional connectivity feature i of the jth sample and y_j denote the class label of this sample ($+1$ for patients and -1 for controls). The Kendall tau correlation coefficient of the functional connectivity feature i can be defined as:

$$\tau_i = \frac{n_c - n_d}{m \times n} \quad (1)$$

where n_c and n_d are the number of concordant and discordant pairs, respectively. Because the relationship between two samples that belong to the same group is not considered, the total number of sample pairs is $m \times n$. For a pair of two-observation data sets $\{x_{ij}, y_j\}$ and $\{x_{ik}, y_k\}$, it is a concordant pair when

$$\mathrm{sgn}(x_{ij} - x_{ik}) = \mathrm{sgn}(y_j - y_k). \quad (2)$$

where sgn( ) is a signum function. Correspondingly, it is a discordant pair when

$$\mathrm{sgn}(x_{ij} - x_{ik}) = -\mathrm{sgn}(y_j - y_k). \quad (3)$$

Thus, a positive correlation coefficient τ_i indicates that the ith functional connectivity coefficient increases in the patient group compared to the control group. A negative τ_i indicates that the ith functional connectivity coefficient decreases in the patient group. The discriminative power was defined as the absolute value of the Kendall tau correlation coefficient. We subsequently ranked features according to their discriminative powers and selected those with coefficients over a threshold as the final feature set for classification.

Since we used a leave-one-out cross-validation strategy to estimate the generalization ability of the classifiers (see below) and feature ranking is based on a slightly different training data set in each iteration of the cross-validation, the final feature set differed slightly from iteration to iteration. Therefore, the contribution of different regions to classification was not evenly distributed, and some regions formed many highly discriminating functional connections with other regions, while some did not form any. Consensus functional connectivity was introduced here, which was defined as the functional connectivity feature appearing in the final feature set of each cross-validation iteration (Dosenbach *et al.*, 2010). Region weight, representing the relative contribution to identification of depressed patients, was denoted by its occurrence number in the consensus functional connections in this study. The consensus functional connectivity discriminative power was denoted by the average of its discriminative powers across all iterations of the cross-validation.

Support vector classification and performance evaluation

When the data set of features with high discriminative power were obtained, support vector machines with linear kernel function were employed to solve the classification problem (Vapnik, 1995; Bishop, 2006). The results were reported with the best parameter setting. Due to our limited number of samples, we used a leave-one-out cross-validation strategy to estimate the generalization ability of our classifier. The performance of a classifier can be quantified using the generalization rate, sensitivity and specificity based on the results of cross-validation. Note that the sensitivity represents the proportion of patients correctly predicted, while the specificity represents the proportion of controls correctly predicted. The overall proportion of samples correctly predicted is evaluated by the generalization rate.

Permutation tests

Some researchers have explored a framework of permutation tests for assessing classifier performance (Golland and Fischl, 2003; Ojala and Garriga, 2010). Choosing the generalization rate as the statistic, permutation tests were employed to estimate the statistical significance of the observed classification accuracy. In permutation testing, the class labels of the training data were randomly permuted prior to training. Cross-validation was then performed on the permuted training set, and the permutation was repeated 10 000 times. It was assumed that a classifier learned reliably from the data when the generalization rate GR_0 obtained by the classifier trained on the real class labels exceeded the 95% confidence interval of the classifier trained on randomly relabelled class labels. For any value of the estimated GR_0, the appropriate P-value $\hat{P}(GR_0)$ represented the probability of observing a classification prediction rate no less than GR_0. We reject the null hypothesis that the classifier could not learn the relationship between the data and the labels reliably and declare that the classifier learned the relationship with a probability of being wrong of at most $\hat{P}(GR_0)$.

Results

Classification results

The classification results indicate that the final correct classification rate of the training data set was 100% using the 550 most discriminating functional connections. Using leave-one-out cross-validation, the linear support vector machine classifier achieved an accuracy of 94.3% (100% for patients, 89.7% for healthy controls, $P < 0.0001$). With the generalization rate as the statistic, the permutation distribution of the estimate is shown in Fig. 1, indicating that the classifier learned the relationship between the data and the labels with a probability of being wrong of <0.0001.

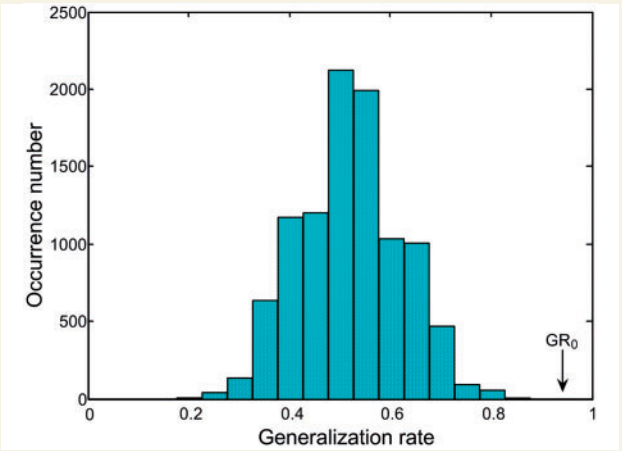

Figure 1 The permutation distribution of the estimate using the linear support vector machine classifier (repetition times: 10 000) when selecting the 550 most discriminating features: *x*- and *y*-labels represent the generalization rate and occurrence number, respectively. GR_0 is the generation rate obtained by the classifier trained on the real class labels. With the generalization rate as the statistic, this figure reveals that the classifier learned the relationship between the data and the labels with a probability of being wrong of <0.0001.

Altered resting-state functional connectivity in major depression

In this investigation, $55.4 \pm 1.0\%$ of the selected functional connections in the cross-validation were diminished in depressed patients compared with healthy controls, and 442 consensus functional connections were identified in the cross-validation (Fig. 2). The brain regions related to consensus functional connectivity are primarily located within: (i) the default mode network (mainly containing the parahippocampal gyrus, anterior cingulate cortex, hippocampus, thalamus, inferior temporal gyrus, posterior cingulate cortex and medial prefrontal cortex), which plays an important role in self-referential activity (Raichle, 2001; Greicius *et al*., 2003); (ii) the affective network (including the amygdala, temporal poles, pallidum, insula and superior temporal gyrus), which is involved in mood regulation and affective processing (Ongür *et al*., 2003; Sheline *et al*., 2010); and (iii) the visual cortical areas (comprising the lingual gyrus, fusiform gyrus, inferior occipital gyrus and calcarine gyrus), which are involved in visual processing (Beckmann *et al*., 2005; Damoiseaux *et al*., 2006; Veer *et al*., 2010). In addition, some consensus functional connections between the cerebellum and the inferior temporal gyrus, hippocampus, parahippocampal gyrus and thalamus in the default mode network,

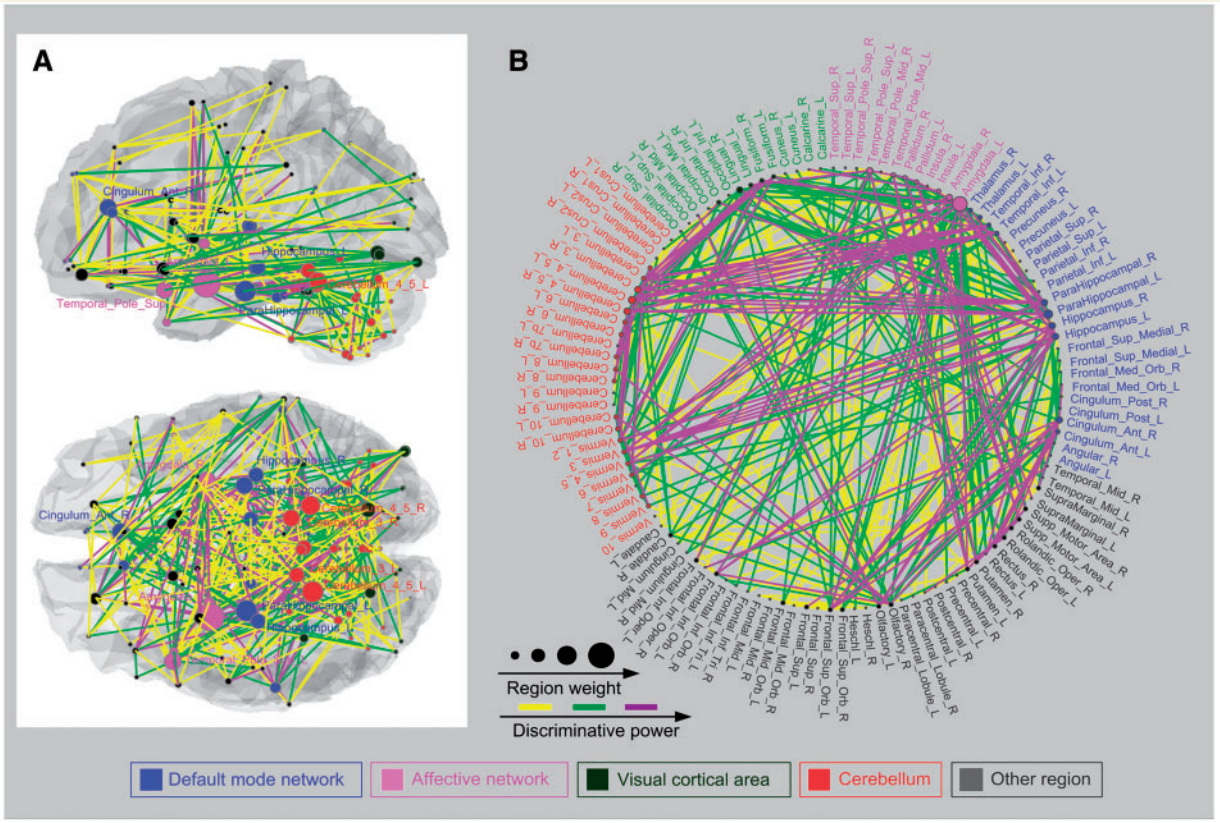

Figure 2 Region weights and the distribution of 442 consensus functional connections. Regions are colour-coded by category. The line colours representing the relative consensus functional connections are scaled with their mean discriminative power in the leave-one-out cross-validation. (**A**) Consensus functional connections demonstrated in left and top view. (**B**) Region weights and consensus functional connections demonstrated in a circle graph.

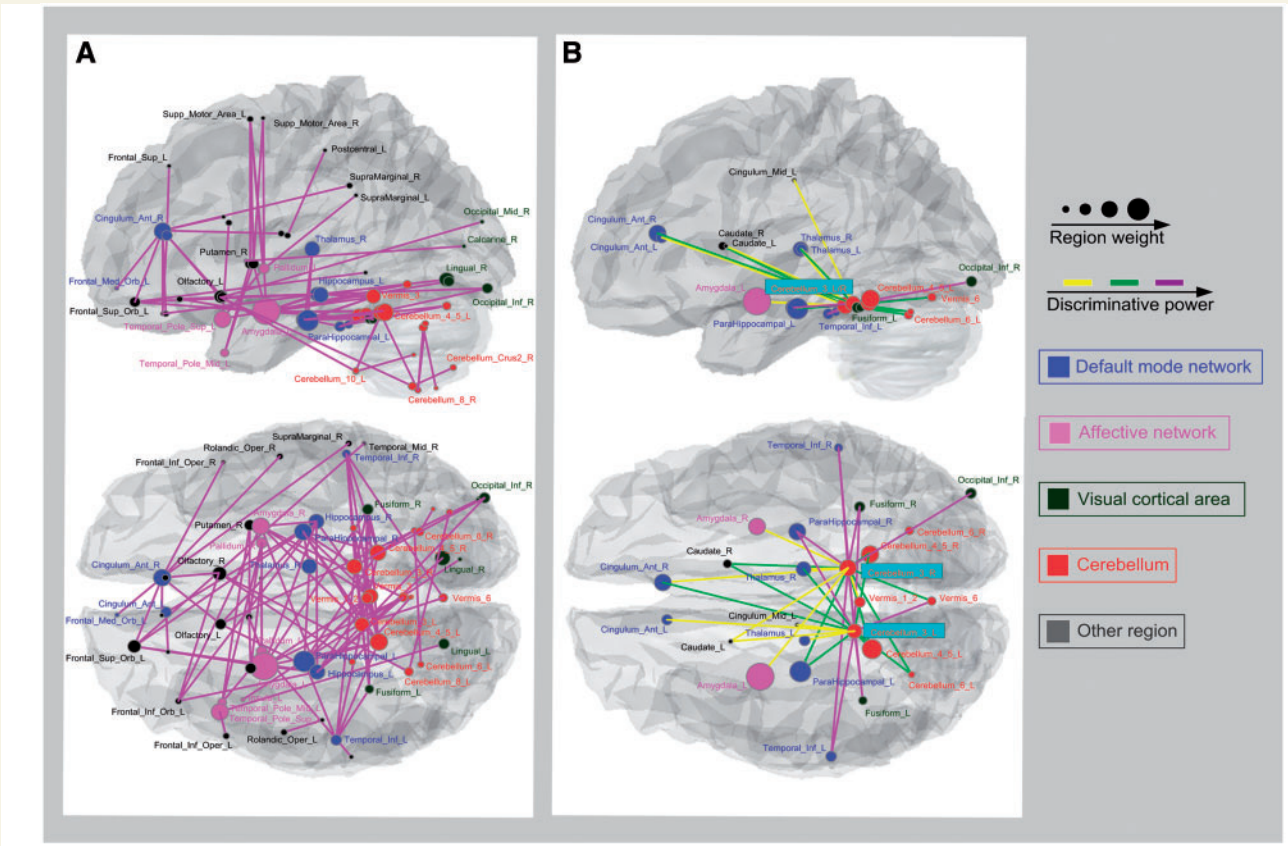

Figure 3 Left and top view of the most discriminating network formed by the top 100 consensus functional connections (**A**) and the consensus functional connectivity network related to the bilateral cerebellar lobule three regions (**B**). Labels indicating brain regions are located at their respective centres of mass. Regions are colour-coded by category. The line colours representing the relative consensus functional connections are scaled with their mean discriminative power in the leave-one-out cross-validation.

as well as the amygdala and temporal poles in the affective network, were unexpected (Fig. 3). The top 100 consensus functional connections are shown in Fig. 3, most of which were also located within or across these resting-state networks.

Brain regions with high discriminative power

For visual representation, the diameter of a sphere representing a region was scaled by the corresponding region weight (Figs 2 and 3). Several brain regions exhibited greater weights than others, i.e. amygdala, anterior cingulate cortex, parahippocampal gyrus and hippocampus. Amygdala exhibited the highest discriminative power, and the functional connections between this region and the prefrontal lobe, visual cortex, other limbic regions and the cerebellum were altered in major depression. Abnormal functional connectivity was also observed between the anterior cingulate cortex and other prefrontal lobe, parahippocampal gyrus and cerebellum. Additionally, functional connections of the parahippocampal gyrus were altered with the inferior temporal gyrus, superior temporal poles, anterior and posterior cingulate cortex, thalamus, fusiform gyrus and cerebellum. Functional connectivity between the hippocampus and the prefrontal lobe, inferior occipital gyrus, amygdala and cerebellum were altered in depressed patients as well.

Discussion

Based on multivariate pattern analysis, this study demonstrated that depressed patients can be distinguished from healthy controls using whole-brain resting-state functional MRI with excellent classification accuracy and sensitivity. Moreover, the majority of the altered functional connections with high discriminative power were located within or across the default mode network, affective network, visual cortical areas and cerebellum. In particular, the amygdala, anterior cingulate cortex, parahippocampal gyrus and hippocampus exhibited high discriminative power in classification.

Altered resting-state networks

Default mode network

Altered functional connectivity was found to be related to the default mode network with regions known to be involved in self-referential activity (Raichle, 2001; Greicius *et al.*, 2003),

such as the bilateral hippocampus/parahippocampal gyrus, anterior cingulate cortex, thalamus, inferior temporal gyrus, posterior cingulate cortex and medial prefrontal cortex. Abnormality of the default mode network in depression is reported in several previous studies (Greicius *et al*., 2007; Bluhm *et al*., 2009; Sheline *et al*., 2010; Zhou *et al*., 2010*b*). In this study, the bilateral hippocampus/parahippocampal gyrus, anterior cingulate cortex, thalamus and inferior temporal gyrus exhibited large region weights. The hippocampus/parahippocampal gyrus is a key structure in the limbic-cortical dysregulation model in major depression (Mayberg, 2003; Seminowicz *et al*., 2004; Drevets *et al*., 2008; Price and Drevets, 2010), and altered functional connections of the hippocampus/parahippocampal gyrus may be related to deficits in emotion-mediated memory formation observed in depression (LaBar and Cabeza, 2006; Savitz and Drevets, 2009). Anterior cingulate cortex, as a critical brain region in emotion processing, has been implicated as a focus of dysfunction in depression (Greicius *et al*., 2007; Sheline *et al*., 2010). Increased connections of the anterior cingulate cortex with other prefrontal cortex and within the default mode network observed here were in keeping with recent studies (Greicius *et al*., 2007). The thalamus has been subjected to intense scrutiny in depression (Greicius *et al*., 2007; Anand *et al*., 2009). Altered connectivity of the thalamus with the prefrontal lobe and the limbic areas may account for the disturbances in autonomic regulations that are associated with depression (Drevets *et al*., 2008). The inferior temporal gyrus is involved in the processing of complex emotional visual stimuli (Geday *et al*., 2001), especially those deeply involved with visual memory (Masahiko and Atsuo, 2002). Abnormal functional connectivity of the inferior temporal gyrus may contribute to working memory dysfunction in depressed patients (Axmacher *et al*., 2008; Parra *et al*., 2010).

Affective network

Abnormalities were found in the resting-state functional connectivity related to the affective network. The affective network in which the amygdala and temporal poles exhibit the greatest region weights is particularly involved in the relationship of emotion/mood to visceral function (Ongür *et al*., 2003; Olson *et al*., 2007; Ding *et al*., 2009). Abnormal connectivity between the amygdala and the hippocampus/parahippocampal gyrus and orbitofrontal cortex were found. All of the above altered connections fall into the limbic-cortical dysregulation model (Mayberg, 2003; Seminowicz *et al*., 2004; Drevets *et al*., 2008; Price and Drevets, 2010) and may negatively affect the regulation of mood and affect (Savitz and Drevets, 2009). In addition, the altered connectivity between temporal poles and the parahippocampal gyrus, as well as the basal ganglia and orbitofrontal cortex, may reflect dysfunctions of visceral monitoring, which is compromised in depression (Sheline *et al*., 2010).

Visual cortical areas

Aberrant connectivity of the visual cortical areas with regions known to be involved in visual processing, such as the lingual gyrus, fusiform gyrus, inferior occipital gyrus and calcarine gyrus, has been demonstrated in this study (Beckmann *et al*., 2005; Damoiseaux *et al*., 2006; Veer *et al*., 2010). The altered functional connections related to the fusiform gyrus, which is involved in the perception of emotions in facial stimuli (Kanwisher *et al*., 1997; Fu *et al*., 2008), may result in the social avoidance observed in depressed patients by participating in negative cognitive models (Yao *et al*., 2009; Liu *et al*., 2010). The abnormality of the resting-state functional connectivity related to the primary visual area, including the occipital cortex and calcarine gyrus and extending into the lingual gyrus, has been reported before (Veer *et al*., 2010) and may be related to impaired selective attention and working memory in major depression (Borkowska and Rybakowski, 2001; Phillips *et al*., 2003; Desseilles *et al*., 2009).

Cerebellum

In the current study, in addition to the aberrant connectivity within itself, altered connections were observed between the cerebellum and the regions in the default mode network and affective network. Using emotional or cognitive tasks with functional MRI, several previous studies have reported abnormalities in the cerebellum in association with depression (Pillay *et al*., 1997; Frodl *et al*., 2010; Liu *et al*., 2010; Guo *et al*., 2011). In this study, the cerebellar connections were primarily altered with the limbic and paralimbic regions comprising the amygdala, hippocampus/parahippocampal gyrus, thalamus and superior temporal poles. To some extent, this result is in accordance with the previous findings that the cerebellum has anatomical connections with the limbic regions, which are involved in mood regulation (Turner *et al*., 2007). The cerebellum may contribute to certain non-motor functions, including emotion and cognitive processing (Dolan, 1998; Schmahmann and Sherman, 1998; Schmahmann and Caplan, 2006; Hu *et al*., 2008; Habas *et al*., 2009; Krienen and Buckner, 2009; O'Reilly *et al*., 2010; Moulton *et al*., 2011). We speculate that the aberrant cerebellar connectivity with the default mode network and affective network may partially underlay emotional and cognitive symptoms seen in major depression.

Reliable identification of major depression

In this study, 100% of 24 depressed patients and 89.7% of 29 healthy control subjects were correctly classified by the linear support vector machine classifier, corresponding to an accuracy of 94.3%. Recently, several brain imaging studies have attempted to distinguish depressed patients from healthy controls (Fu *et al*., 2008; Costafreda *et al*., 2009; Craddock *et al*., 2009). However, to the best of our knowledge, no previous studies have achieved such a high level of classification accuracy, considering the sample size. Thus, we believe that this classifier detected the reliable population differences between depressed patients and healthy controls (Golland and Fischl, 2003). Furthermore, choosing the generalization rate as the statistic, the statistical significance of the observed classification accuracies was estimated by permutation testing. The results demonstrate that the linear support vector machine classifier learned the relationship between the data and the labels with a probability of being wrong of <0.0001. In other words, this multivariate pattern analysis method reliably captured the disorder-related resting-state functional connectivity patterns.

Pattern classification of functional MRI data is a challenging task, due to the high dimensionality of the data, individual variability, noisy measurements and small available sample sizes. The present study demonstrates that resting-state connectivity patterns can distinguish depressed patients from controls with a high degree of accuracy. However, some issues that may potentially influence classifier performance should be addressed here. Brain atlas selection may have an impact on functional connectivity measurements (Smith *et al*., 2011). Functionally defined regions of interest have recently been suggested in whole-brain connectivity analysis (Shirer *et al*., 2012). Using the 90 functional regions of interest defined by Shirer *et al*. (2012), the support vector machine classifier performed with a classification accuracy of 92.5%. We speculate that more accurate functionally defined regions of interest distributed throughout the entire brain may improve the classification performance.

Limitations and future directions

Although the classification results of this study using resting-state functional connectivity are encouraging, there are still limitations related to sample size, scanner variability and the lack of a large independent data set with which to test our methods and confirm the findings. Therefore, it is important to confirm the classification results with a larger sample size and multicentre imaging data in the future. Some physiological noises, such as cardiac and respiratory rates, can alias into the low-frequency domain of functional MRI signals (Strother, 2006; Murphy *et al*., 2009). However, cardiac and respiratory rates were not collected during the scans in this study, and the impact of these physiological noises on classifier performance remains to be determined. Additional neuroimaging evidence, such as structural abnormality other than resting-state functional connectivity, is needed as a synthesized biomarker for more reliable clinical diagnosis of this complex disorder. The automated anatomical labelling atlas, including 116 regions, covers the entire cerebrum and the cerebellum but excludes the brainstem, which may be central to monoaminergic hypotheses in major depression (Drevets *et al*., 2007); clearly, the functional connectivity of the brainstem should be investigated in the future. In addition, an assessment of the relationship between the consensus functional connections and the clinical variables is needed to delineate the consensus functional connections and to confirm that consensus functional connections prove reliable within depression.

Conclusion

This study demonstrates that multivariate pattern analysis methods can identify major depressive individuals from healthy controls based on resting-state functional MRI with 94.3% classification accuracy. The majority of the most discriminating functional connections were located within or across the default mode network, affective network, visual cortical areas and cerebellum, thereby indicating that the disease-related resting-state network alterations may give rise to a portion of the complex of emotional and cognitive disturbances in major depression. Moreover, the amygdala, anterior cingulate cortex, parahippocampal gyrus and hippocampus may play important roles in the pathophysiology of this disorder. Future investigations are needed to combine whole-brain resting-state functional connectivity with other neuroimaging evidence, such as structural abnormality as a synthesized biomarker, for more reliable clinical diagnosis.

Acknowledgements

We thank the volunteers and patients for their participation in the study and the three anonymous referees for their insightful comments and suggestions.

Funding

National Basic Research Programme of China (Grant No. 2011CB707802) and National Science Foundation of China (Grant Nos 60835005, 61003202, 90820304).

References

Anand A, Li Y, Wang Y, Lowe MJ, Dzemidzic M. Resting state corticolimbic connectivity abnormalities in unmedicated bipolar disorder and unipolar depression. Psychiatry Res-Neuroim 2009; 171: 189–98.

Anand A, Li Y, Wang Y, Wu JW, Gao SJ, Bukhari L, et al. Activity and connectivity of brain mood regulating circuit in depression: a functional magnetic resonance study. Biol Psychiatry 2005; 57: 1079–88.

APA. Diagnostic and statistical manual of mental disorders. 4th edn. Washington, DC: American Psychiatric Press; 2000.

Ardekani BA, Tabesh A, Sevy S, Robinson DG, Bilder RM, Szeszko PR. Diffusion tensor imaging reliably differentiates patients with schizophrenia from healthy volunteers. Hum Brain Mapp 2011; 32: 1–9.

Axmacher N, Schmitz DP, Wagner T, Elger CE, Fell J. Interactions between medial temporal lobe, prefrontal cortex, and inferior temporal regions during visual working memory: a combined intracranial EEG and functional magnetic resonance imaging study. J Neurosci 2008; 28: 7304–12.

Beckmann CF, DeLuca M, Devlin JT, Smith SM. Investigations into resting-state connectivity using independent component analysis. Philos Trans R Soc Lond B Biol Sci 2005; 360: 1001–13.

Bishop CM. Pattern recognition and machine learning. New York: Springer; 2006.

Biswal BB, Mennes M, Zuo X-N, Gohel S, Kelly C, Smith SM, et al. Toward discovery science of human brain function. Proc Natl Acad Sci USA 2010; 107: 4734–9.

Bluhm R, Williamson P, Lanius R, Théberge J, Densmore M, Bartha R, et al. Resting state default-mode network connectivity in early depression using a seed region-of-interest analysis: decreased connectivity with caudate nucleus. Psychiatry Clin Neurosci 2009; 63: 754–61.

Borkowska A, Rybakowski JK. Neuropsychological frontal lobe tests indicate that bipolar depressed patients are more impaired than unipolar. Bipolar Disord 2001; 3: 88–94.

Buckner RL. Human functional connectivity: new tools, unresolved questions. Proc Natl Acad Sci USA 2010; 107: 10769–70.

Costafreda SG, Chu C, Ashburner J, Fu CHY. Prognostic and diagnostic potential of the structural neuroanatomy of depression. PloS ONE 2009; 4: e6353.

Craddock RC, Holtzheimer PE III, Hu XP, Mayberg HS. Disease state prediction from resting state functional connectivity. Magn Reson Med 2009; 62: 1619–28.

Damoiseaux JS, Rombouts S, Barkhof F, Scheltens P, Stam CJ, Smith SM, et al. Consistent resting-state networks across healthy subjects. Proc Natl Acad Sci USA 2006; 103: 13848–53.
Davidson RJ, Lewis DA, Alloy LB, Amaral DG, Bush G, Cohen JD, et al. Neural and behavioral substrates of mood and mood regulation. Biol Psychiatry 2002; 52: 478–502.
Desikan RS, Cabral HJ, Hess CP, Dillon WP, Glastonbury CM, Weiner MW, et al. Automated MRI measures identify individuals with mild cognitive impairment and Alzheimer's disease. Brain 2009; 132: 2048–57.
Desseilles M, Balteau E, Sterpenich V, Dang-Vu TT, Darsaud A, Vandewalle G, et al. Abnormal neural filtering of irrelevant visual information in depression. J Neurosci 2009; 29: 1395–403.
Ding SL, Van Hoesen GW, Cassell MD, Poremba A. Parcellation of human temporal polar cortex: a combined analysis of multiple cytoarchitectonic, chemoarchitectonic, and pathological markers. J Comp Neurol 2009; 18: 595–623.
Dolan RJ. A cognitive affective role for the cerebellum. Brain 1998; 121: 545–6.
Dosenbach NUF, Nardos B, Cohen AL, Fair DA, Power JD, Church JA, et al. Prediction of Individual Brain Maturity Using fMRI. Science 2010; 329: 1358–61.
Drevets WC. Neuroimaging abnormalities in the amygdala in mood disorders. Ann NY Acad Sci 2003; 985: 420–44.
Drevets WC, Price JL, Furey ML. Brain structural and functional abnormalities in mood disorders: implications for neurocircuitry models of depression. Brain Struct Funct 2008; 213: 93–118.
Drevets WC, Thase ME, Moses-Kolko EL, Price J, Frank E, Kupfer DJ, et al. Serotonin-1A receptor imaging in recurrent depression: replication and literature review. Nucl Med Biol 2007; 34: 865–77.
Fair DA, Cohen AL, Dosenbach NUF, Church JA, Miezin FM, Barch DM, et al. The maturing architecture of the brain's default network. Proc Natl Acad Sci USA 2008; 105: 4028–32.
First MB, Spitzer RL, Gibbon M. Structured clinical Interview for DSM-IV axis 1 disorder-patient edition(SCID-I/P). New York: New York State Psychiatric Institute; 1995.
Fox MD, Corbetta M, Snyder AZ, Vincent JL, Raichle ME. Spontaneous neuronal activity distinguishes human dorsal and ventral attention systems. Proc Natl Acad Sci USA 2006; 103: 10046–51.
Fox MD, Zhang DY, Snyder AZ, Raichle ME. The global signal and observed anticorrelated resting state brain networks. J Neurophysiol 2009; 101: 3270–83.
Frodl T, Bokde ALW, Scheuerecker J, Lisiecka D, Schoepf V, Hampel H, et al. Functional connectivity bias of the orbitofrontal cortex in drug-free patients with major depression. Biol Psychiatry 2010; 67: 161–7.
Fu CHY, Mourao-Miranda J, Costafrecla SG, Khanna A, Marquand AF, Williams SC, et al. Pattern classification of sad facial processing: toward the development of neurobiological markers in depression. Biol Psychiatry 2008; 63: 656–62.
Geday J, Ehlersf L, Boldsen AS, Gjedde A. The inferior temporal and orbitofrontal cortex in analysing emotional pictures. Neuroimage 2001; 13: S406.
Golland P, Fischl B. Permutation tests for classification: towards statistical significance in image-based studies. Inf Process Med Imaging 2003; 2732: 330–41.
Greicius MD. Resting-state functional connectivity in neuropsychiatric disorders. Curr Opin Neurol 2008; 21: 424–30.
Greicius MD, Flores BH, Menon V, Glover GH, Solvason HB, Kenna H, et al. Resting-state functional connectivity in major depression: abnormally increased contributions from subgenual cingulate cortex and thalamus. Biol Psychiatry 2007; 62: 429–37.
Greicius MD, Krasnow B, Reiss AL, Menon V. Functional connectivity in the resting brain: a network analysis of the default mode hypothesis. Proc Natl Acad Sci USA 2003; 100: 253–8.
Greicius MD, Srivastava G, Reiss AL, Menon V. Default mode network activity distinguishes Alzheimer's disease from healthy aging: evidence from functional MRI. Proc Natl Acad Sci USA 2004; 101: 4637–42.
Guo WB, Liu F, Xue ZM, Yu Y, Ma CQ, Tan CL, et al. Abnormal neural activities in first-episode, treatment-naïve, short-illness-duration, and treatment-response patients with major depressive disorder: a resting-state fMRI study. J Affect Disord 2011; 135: 326–31.
Guy W. Clinical global impressions: in ECDEU assessment manual for psychopharmacology. Revised DHEW Pub. (ADM). Rockville, MD: National Institute for Mental Health; 1976.
Guyon I, Elisseeff A. An introduction to variable and feature selection. J Mach Learn Res 2003; 3: 1157–82.
Habas C, Kamdar N, Nguyen D, Prater K, Beckmann CF, Menon V, et al. Distinct cerebellar contributions to intrinsic connectivity networks. J Neurosci 2009; 29: 8586–94.
Hamilton M. The assessment of anxiety states by rating. Br J Med Psychol 1959; 32: 50–5.
Hamilton M. A rating scale for depression. J Neurol Neurosurg Psychiatry 1960; 23: 56–62.
Hu D, Shen H, Zhou Z. Functional asymmetry in the cerebellum: a brief review. Cerebellum 2008; 7: 304–13.
Kanwisher N, McDermott J, Chun MM. The fusiform face area: a module in human extrastriate cortex specialized for face perception. J Neurosci 1997; 17: 4302–11.
Kelly RE, Alexopoulos GS, Wang Z, Gunning FM, Murphy CF, Morimoto SS, et al. Visual inspection of independent components: defining a procedure for artifact removal from fMRI data. J Neurosci Methods 2010; 189: 233–45.
Kendall MG, Jean DG. Rank correlation methods. New York: Oxford University Press; 1990.
Klöppel S, Stonnington CM, Chu C, Draganski B, Scahill RI, Rohrer JD, et al. Automatic classification of MR scans in Alzheimer's disease. Brain 2008; 131: 681–9.
Krienen FM, Buckner RL. Segregated fronto-cerebellar circuits revealed by intrinsic functional connectivity. Cereb Cortex 2009; 19: 2485–97.
LaBar KS, Cabeza R. Cognitive neuroscience of emotional memory. Nat Rev Neurosci 2006; 7: 54–64.
Liu Y, Hu D, Zhou Z, Shen H, Wang X. fMRI noise reduction based on canonical correlation analysis and surrogate test. IEEE J Sel Top Sign Proces 2008a; 6: 870–8.
Liu Y, Liang M, Zhou Y, He Y, Hao Y, Song M, et al. Disrupted small-world networks in schizophrenia. Brain 2008b; 131: 945–61.
Liu ZF, Xu C, Xu Y, Wang YF, Zhao B, Lv YT, et al. Decreased regional homogeneity in insula and cerebellum: a resting-state fMRI study in patients with major depression and subjects at high risk for major depression. Psychiatry Res 2010; 182: 211–5.
Maldjian JA, Laurienti PJ, Burdette JB, Kraft RA. An automated method for neuroanatomic and cytoarchitectonic atlas-based interrogation of fMRI data sets. Neuroimage 2003; 19: 1233–9.
Masahiko M, Atsuo S. Computational modeling of pair-association memory in inferior temporal cortex. Cogn Brain Res 2002; 13: 169–78.
Mayberg HS. Limbic-cortical dysregulation: a proposed model of depression. J Neuropsychiatry Clin Neurosci 1997; 9: 471–81.
Mayberg HS. Modulating dysfunctional limbic-cortical circuits in depression: towards development of brain-based algorithms for diagnosis and optimised treatment. Br Med Bull 2003; 65: 193–207.
Mesulam M-M. From sensation to cognition. Brain 1998; 121: 1013–52.
Moulton EA, Elman I, Pendse G, Schmahmann J, Becerra L, Borsook D. Aversion-related circuitry in the cerebellum: responses to noxious heat and unpleasant images. J Neurosci 2011; 31: 3795–804.
Murphy K, Birn RM, Handwerker DA, Jones TB, A, Bandettini P. The impact of global signal regression on resting state correlations: are anti-correlated networks introduced? Neuroimage 2009; 44: 893–905.
Ojala M, Garriga GC. Permutation tests for studying classifier performance. J Mach Learn Res 2010; 11: 1833–63.
Olson IR, Plotzker A, Ezzyat Y. The Enigmatic temporal pole: a review of findings on social and emotional processing. Brain 2007; 130: 1718–31.
Ongür D, Ferry AT, Price JL. Architectonic subdivision of the human orbital and medial prefrontal cortex. J Comp Neurol 2003; 460: 425–49.

O'Reilly JX, Beckmann CF, Tomassini V, Ramnani N, Johansen-Berg H. Distinct and overlapping functional zones in the cerebellum defined by resting state functional connectivity. Cereb Cortex 2010; 20: 953–65.

Parra MA, Abrahams S, Logie RH, Sala SD. Visual short-term memory binding in Alzheimer's disease and depression. J Neurol 2010; 257: 1160–9.

Pereira F, Mitchell T, Botvinick M. Machine learning classifiers and fMRI: a tutorial overview. Neuroimage 2009; 45: S199–209.

Phillips ML, Drevets WC, Rauch SL, Lane R. Neurobiology of emotion perception II: the neural basis of normal emotion perception. Biol Psychiatry 2003; 54: 504–14.

Pillay SS, Yurgelun-Todd DA, Bonello CM, Lafer B, Fava M, Renshaw PF. A quantitative magnetic resonance imaging study of cerebral and cerebellar grey matter volume in primary unipolar major depression: relationship to treatment response and clinical severity. Biol Psychiatry 1997; 42: 79–84.

Price JL, Drevets WC. Neurocircuitry of mood disorders. Neuropsychopharmacology 2010; 35: 192–216.

Raichle ME. A default mode of brain function. Proc Natl Acad Sci USA 2001; 98: 676–82.

Savitz J, Drevets WC. Bipolar and major depressive disorder: neuroimaging the develop mental-degenerative divide. Neurosci Biobehav Rev 2009; 33: 699–771.

Schmahmann JD, Caplan D. Cognition, emotion and the cerebellum. Brain 2006; 129: 290–2.

Schmahmann JD, Doyon J, McDonald D, Holmes C, Lavoie K, Hurwitz AS, et al. Three-dimensional MRI atlas of the human cerebellum in proportional stereotaxic space. Neuroimage 1999; 10: 233–60.

Schmahmann JD, Sherman JC. The cerebellar cognitive affective syndrome. Brain 1998; 121: 561–79.

Seidman LJ, Valera EM, Bush G. Brain function and structure in adults with attention-deficit/hyperactivity disorder. Psychiatr Clin North Am 2004; 27: 323–47.

Seminowicz DA, Mayberg HS, McIntosh AR, Goldapple K, Kennedy S, Segal Z, et al. Limbic-frontal circuitry in major depression: a path modeling metanalysis. Neuroimage 2004; 22: 409–18.

Sheline YI, Price JL, Yan ZZ, Mintun MA. Resting-state functional MRI in depression unmasks increased connectivity between networks via the dorsal nexus. Proc Natl Acad Sci USA 2010; 107: 11020–5.

Shen H, Wang L, Liu Y, Hu D. Discriminative analysis of resting-state functional connectivity patterns of schizophrenia using low dimensional embedding of fMRI. Neuroimage 2010; 49: 3110–21.

Shirer WR, Ryali S, Rykhlevskaia E, Menon V, Greicius MD. Decoding subject-driven cognitive states with whole-brain connectivity patterns. Cereb Cortex 2012; 22: 158–65.

Smith SM, Miller KL, Salimi-Khorshidi G, Webster M, Beckmann CF, Nichols TE, et al. Network modelling methods for FMRI. Neuroimage 2011; 54: 875–91.

Strother SC. Evaluating fMRI preprocessing pipelines: review of preprocessing steps for BOLD fMRI. IEEE Eng Med Biol Mag 2006; 27–41.

Turner BM, Paradiso S, Marvel CL, Pierson R, Ponto LLB, Hichwa RD, et al. The cerebellum and emotional experience. Neuropsychologia 2007; 45: 1331–41.

Tzourio-Mazoyer N, Landeau B, Papathanassiou D, Crivello F, Etard O, Delcroix N, et al. Automated anatomical labeling of activations in SPM using a macroscopic anatomical parcellation of the MNI MRI single-subject brain. Neuroimage 2002; 15: 273–89.

Van den Heuvel MP, Hulshoff Pol HE. Exploring the brain network: a review on resting-state fMRI functional connectivity. Eur Neuropsychopharmacol 2010; 20: 519–34.

Vapnik V. The natures of statistical learning theory. New York: Springer-Verlag; 1995.

Veer IM, Beckmann CF, van Tol M-J, Ferrarini L, Milles J, Veltman DJ, et al. Whole brain resting-state analysis reveals decreased functional connectivity in major depression. Front Syst Neurosci 2010; 4: 1–10.

Whitfield-Gabrieli S, Thermenos HW, Milanovic S, Tsuang MT, Faraone SV, McCarley RW, et al. Hyperactivity and hyperconnectivity of the default network in schizophrenia and in first-degree relatives of persons with schizophrenia. Proc Natl Acad Sci USA 2009; 106: 1279–84.

Yao ZJ, Wang L, Lu Q, Liu HY, Teng GJ. Regional homogeneity in depression and its relationship with separate depressive symptom clusters: a resting-state fMRI study. J Affect Disord 2009; 115: 430–8.

Zhou J, Greicius MD, Gennatas ED, Growdon ME, Jang JY, Rabinovici GD, et al. Divergent network connectivity changes in behavioural variant frontotemporal dementia and Alzheimer's disease. Brain 2010a; 133: 1352–67.

Zhou Y, Yu CS, Zheng H, Liu Y, Song M, Qin W, et al. Increased neural resources recruitment in the intrinsic organization in major depression. J Affect Disord 2010b; 121: 220–30.